analytical chemistry

Article

pubs.acs.org/ac

Sensitive Electrochemiluminescence Detection of c-Myc mRNA in Breast Cancer Cells on a Wireless Bipolar Electrode

Mei-Sheng Wu, Guang-sheng Qian, Jing-Juan Xu,* and Hong-Yuan Chen

State Key Laboratory of Analytical Chemistry for Life Science, School of Chemistry and Chemical Engineering, Nanjing University, Nanjing 210093, China

Supporting Information

ABSTRACT: We report an ultrasensitive wireless electrochemiluminescence (ECL) protocol for the detection of a nucleic acid target in tumor cells on an indium tin oxide bipolar electrode (BPE) in a poly(dimethylsiloxane) microchannel. The approach is based on the modification of the anodic pole of the BPE with antisense DNA as the recognition element, $Ru(bpy)_3^{2+}$-conjugated silica nanoparticles (RuSi@$Ru(bpy)_3^{2+}$) as the signal amplification tag, and reporter DNA as a reference standard. It employs the hybridization-induced changes of RuSi@$Ru(bpy)_3^{2+}$ ECL efficiency for the specific detection of reporter DNA released from tumor cells. Prior to ECL detection, tumor cells are transfected with CdSe@ZnS quantum dot (QD)−antisense DNA/reporter DNA conjugates. Upon the selective binding of antisense DNA probes to intracellular target mRNA, reporter DNA will be released from the QDs, which indicates the amount of the target mRNA. The proof of concept is demonstrated using a proto-oncogene c-Myc mRNA in MCF-7 cells (breast cancer cell line) as a model target. The wireless ECL biosensor exhibited excellent ECL signals which showed a good linear range over 2×10^{-16} to 1×10^{-11} M toward the reporter DNA detection and could accurately quantify c-Myc mRNA copy numbers in living cells. C-Myc mRNA in each MCF-7 cell and LO2 cell was estimated to be 2203 and 13 copies, respectively. This wireless ECL strategy provides great promise in a miniaturized device and may facilitate the achievement of point of care testing.

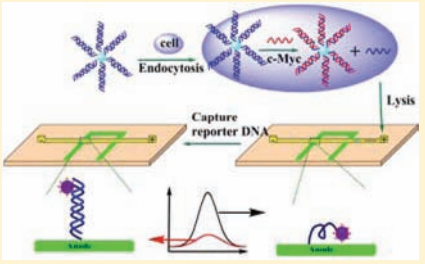

Highly sensitive detection of specific ribonucleic acid (RNA) transcripts is crucially important for identification of the subtypes of disease and clinical diagnosis. Quantification of the expression levels of a particular mRNA via the hybridization of mRNA with a complementary sequence is widely used in various types of biosensors with fluorescence,[1] electrochemical,[2] and electrochemiluminescence[3−5] (ECL) readouts and amplified by real-time polymerase chain reaction (RT-PCR),[2,3] cDNA microarray analysis,[1] and nucleic acid sequence based amplification.[4,5] Although these biosensors can detect mRNA expression in bulk samples, they require calibration with known concentrations of pure mRNA, which involves labor-intensive and time-consuming procedures. Besides, they are capable of investigating mRNA-associated cell variation because cells are lysed to release mRNA. Furthermore, RNA is known to be extremely labile and susceptible to degradation by extracting RNA from cells/tissues in an environment inhibitory to nucleases, which would likely influence the quantitative accuracy. Alternative approaches for endogenous mRNA analysis, such as in situ hybridization and molecular beacon, have been used for mRNA measurements within living cells based on fluorescence resonance energy transfer (FRET).[6,7] These quantitative approaches largely obviate the need for precise knowledge of the concentration of mRNA. Nevertheless, the application of these approaches is significantly limited by the light scattering in the sample and the excitation source fluctuations, and such fluorescence-linked assays often require the correction of fluorescence intensity.[8]

Among the diverse mRNA detection techniques, the ECL technique has been developed as one of the most versatile methods for the detection of biological recognition events of interest due to its high sensitivity, good temporal and spatial control, and simplified optical setup.[9] It is immune to interferences from luminescent impurities and the scattered light ECL method in fluorescence assays because no excitation source is required. Recently, ECL detection on bipolar electrodes (BPEs) has emerged as a sensitive, high-throughput, and low-cost approach.[10−12] BPEs are usually set up in microfluidic chips. The potential difference (E_{elec}) on the BPE is obtained by applying a potential at the two ends of a microchannel (E_{tot}). When it reaches a critical value, the redox reaction takes place at both poles of the BPE simultaneously. A typical ECL system on a BPE uses $Ru(bpy)_3^{2+}$ as the ECL emission species and tripropylamine (TPA) as a coreactant. In this strategy, $Ru(bpy)_3^{2+}$ and TPA are oxidized at the anodic pole of BPE. Compared with other detection methods, this biosensing platform possesses the advantages of concentration enrichment, high sensitivity, low cost, portable sensor system, and no need for a direct external connection to the electrode, which facilitates its integration in miniaturized devices. Recently, our laboratory has reported the development of a wireless ECL device for sensitive detection of folic acid and a

Received: April 13, 2012
Accepted: May 21, 2012
Published: May 21, 2012

   dx.doi.org/10.1021/ac3009912 | *Anal. Chem.* 2012, 84, 5407−5414

cell surface receptor based on the quenching effect of folic acid on $Ru(bpy)_3^{2+}$ ECL emission on a microband BPE.[12] On the basis of specific recognition between folic acid and a folate receptor on a cell membrane, this microfluidic chip−ECL system is successfully applied for detecting the level of folate receptor on a human cervical tumor (HL-60) cell. For the purpose of quantification of the expression levels of particular mRNA in cells, it is necessary to further develop special recognition surfaces and devices for intracellular marker measurement.

In this work, we report the development of a wireless on-chip ECL biosensor to achieve sensitive monitoring of c-Myc mRNA using MCF-7 cells as a model. The c-Myc gene is a proto-oncogene which plays a crucial role in cell proliferation, cellular transformation, and apoptosis.[13] Besides, studies indicate that c-Myc mRNA is important in the development and progression of breast cancer, in that overexpression of c-Myc mRNA is found in most breast cancer. It is a hot topic to investigate the viability of preventing cancer growth by cleaving or degrading the c-Myc mRNA. Thus, in this study, we detect the expression level of c-Myc mRNA in a breast cancer cell line (MCF-7 cells) and investigate whether specifically decreasing the level of c-Myc mRNA in MCF-7 cells might result in the inhibition of cell growth. In an attempt to protect RNA-based biosensors from degradation, we replace RNA bases with their more degradation-resistant DNA equivalents. Reporter DNA is hybridized with antisense DNA on CdSe@ZnS quantum dots (QDs) and then transfected into living cells via an endocytic pathway. Once internalized into cells, cellular c-Myc mRNA hybridizes with antisense DNA and therefore obstructs the translation of c-Myc mRNA into protein by base pairing. Meanwhile, the reporter DNA liberated from lysis cells is detected by an ECL biosensor. Here, the ECL biosensor is fabricated by conjugating ECL probe labeled antisense DNA on one arm of a U-shaped indium tin oxide (ITO) BPE. The interaction of reporter DNA with antisense DNA causes the separation of the ECL probe away from the electrode surface, thus resulting in a decrease of the ECL signal. Here, RuSi@$Ru(bpy)_3^{2+}$ was used as the ECL probe to amplify the signal. Recently, $Ru(bpy)_3^{2+}$-doped silica (RuSi) nanospheres have been widely used in bioanalysis because of their biocompatibility, chemical stability, and easy surface modification.[14] The silica matrixes can resist ECL tag release and improve their stabilities. However, silica matrixes could also inhibit the electron transfer from $Ru(bpy)_3^{2+}$ to the electrode. In this paper, benefiting from the large surface area of RuSi which could covalently bind a large amount of $Ru(bpy)_3^{2+}$ and then enhance ECL sensitivity greatly, we fabricated $Ru(bpy)_3^{2+}$-coated RuSi nanoparticles (NPs; RuSi@$Ru(bpy)_3^{2+}$). The ECL signal observed by the application of the RuSi@$Ru(bpy)_3^{2+}$ probe was enhanced 24- and 12-fold compared to those of $Ru(bpy)_3^{2+}$ and RuSi NPs, respectively. The ECL biosensor exhibited excellent sensitivity toward DNA detection. Uniquely, this wireless on-chip ECL biosensor does not require calibration with pure mRNA because it uses the reporter DNA probe as an internal standard. In addition, in the signal amplification system, the number of target molecules is not altered, and as a result, it reduces the false positives because of cross-contamination, simplifies the quantitative assays, and offers highly sensitive detection of mRNA.

EXPERIMENTAL SECTION

Materials. *N*-[3-(Dimethylamino)propyl]-*N*′-ethylcarbodiimide hydrochloride (EDC), single-stranded DNA binding protein (SSB), DNase I, (3-aminopropyl)triethoxysilane (APTES), *N*-hydroxysuccinimide (NHS), sodium dodecyl sulfate (SDS), $Ru(bpy)_3^{2+}$−*N*-hydroxysuccinimide (NHS), and TPA were obtained from Sigma-Aldrich. MCF-7 cells (breast cancer cell line) were from Gulou Hospital (Nanjing, China). LO2 cells (normal liver cells) were from KeyGEN Biotech (Nanjing, China). Dulbecco's modified Eagle's medium (DMEM; Gibco Invitrogen Corp., Grand Island, NY), fetal bovine serum (FBS; Gibco Invitrogen Corp.), penicillin, and streptomycin were purchased from KeyGEN Biotech (Nanjing, China). A 96-well cell culture plate was purchased from Corning Inc. (Corning, NY). ITO-coated (thickness ∼100 nm, resistance ∼10 Ω/square) aluminosilicate glass slides were purchased from CSG (Shenzhen, China). Sylgard 184 (including poly(dimethylsiloxane) (PDMS) monomer and curing agent) was from Dow Corning (Midland, MI). SG-2506 borosilicate glass (with a 145 nm thick chrome film and a 570 nm thick positive S-1805 type photoresist was from Changsha Shaoguang Chrome Blank Co. Ltd. Phosphate-buffered saline (PBS; pH 7.4, 10 mM) contained 137 mM NaCl, 2.7 mM KCl, 87.2 mM Na_2HPO_4, and 14.1 mM KH_2PO_4. The ECL detection solution was 0.1 M PBS buffer solution (pH 7.4) containing 1 M NaCl and 1 mM TPA. All solutions were prepared using Millipore (model Milli-Q) purified water and stored at 4 °C in a refrigerator. All the other chemicals were of analytical grade.

All of the DNA probes were synthesized by Sangon Biotech Co. Ltd. (Shanghai, China). Antisense DNA probe: 5′-NH_2-$(CH_2)_6$-CTC GGT TGT CCT GGA TGA TGT TTT CAA CC-$(CH_2)_6$-NH_2-3′). Reporter DNA probe: 5′-**AAA ACA TCA TCA TCC AGG A**-3′.

Instruments. ECL signals were measured with an MPI-E electrochemiluminescence analyzer (Xi'An Remax Electronic Science & Technology Co. Ltd., Xi'An, China, 350−650 nm). A DMIRE2 inverted fluorescence microscope (Leica, Germany) equipped with a DP71 charge-coupled device (CCD; Olympus, Japan) was applied for cell imaging, the results of which were analyzed by Image-Pro Plus (IPP) 6.0 software. A Hitachi/Roche System Cobas 6000 (Tokyo, Japan) was used to examine the effect of CdSe@ZnS−dsDNA on the growth of MCF-7 cells. A U-shaped ITO microelectrode embedded in a microchannel was used for wireless ECL detection. Fluorescence spectra were obtained on an RF-540 spectrophotometer (Shimadzu Co). The UV−vis absorption spectra were obtained on a Shimadzu UV-3600 UV−vis−NIR photospectrometer (Shimadzu Co.).

Preparation of CdSe@ZnS−dsDNA Conjugates. The preparation of CdSe@ZnS was achieved according to previous reports.[15,16] Briefly, Se powder was premixed with 50 mL of a 0.015 g Na_2SO_3 solution under constant stirring at 100 °C for 2 h to prepare the Na_2SeSO_3 solution (solution A). A 0.055 g sample of $CdCl_2{\cdot}2.5H_2O$ and 52 μL of MPA were added to 50 mL of ultrapure water, followed by addition of 1 M $NH_3{\cdot}H_2O$ until the pH value was 9.0 (solution B). Then solution A was added into solution B under continuous stirring at 100 °C for about 2 h, and the reaction solution was cooled naturally to room temperature. For the preparation of CdSe/ZnS core/shell QDs, 3 mL of 2.4 mM Na_2S solution and 3 mL of 3.2 mM $Zn(OOCH_2CH_3)_2$ solution were added to the above mixture

dx.doi.org/10.1021/ac3009912 | Anal. Chem. 2012, 84, 5407−5414

under constant stirring at 60 °C for 5 h, followed by centrifuging, washing three times with ethanol and ultrapure water, and redispersing in ultrapure water.

CdSe@ZnS QDs were incubated with EDC and NHS (1:2) for 30 min under gentle stirring. Then 1×10^{-7} M amine-terminated antisense DNA was introduced into the above solution under gentle mixing for 4 h. The solution containing antisense DNA functionalized QDs was centrifuged and washed with PBS. Reporter DNA (1×10^{-7} M) was added into the as-prepared QD−antisense DNA and allowed to hybridize for 3 h at 37 °C to form CdSe@ZnS−dsDNA conjugates.

Cell Uptake, Viability, and Lysis. Cells were cultured in DMEM medium containing 10% fetal calf serum, penicillin (100 mg/mL), and streptomycin (100 mg/mL) in a 5% CO_2 incubator. Cells were seeded into each well of a 96-well plate and grown for 2 days prior to transfection. Cells were transfected with CdSe@ZnS−dsDNA conjugates in fresh medium and harvested after 3 h. 3-(4,5-Dimethylthiazol-2-yl)-2,5-diphenyltetrazolium bromide (MTT) assay was used to evaluate the viability of MCF-7 cells. CdSe@ZnS−dsDNA transfected MCF-7 cells were stained with MTT for 4 h at 37 °C. Subsequently, the medium was removed, and 100 μL of dimethyl sulfoxide (DMSO) was added to each well to dissolve the precipitate. The final solution was measured using a Hitachi/Roche System Cobas 6000 (Tokyo, Japan) at 490 nm. The relative cell viability (%) was calculated by $(A_{test}/A_{control}) \times 100$.

After the transfection of cells, the cell pellet was washed two times with PBS. A 50 μL sample of 1% (w/v) SDS was added to the cell pellet and incubated for 30 min at 37 °C, and then the reporter DNA was released from the cells.[17]

Synthesis and Modification of the RuSi@Ru(bpy)$_3^{2+}$ Probe. The RuSi@ $Ru(bpy)_3^{2+}$ probe was prepared by the following procedure.[14] First, 1.77 mL of Triton X-100, 7.5 mL of cyclohexane, 1.8 mL of 1-hexanol, and 340 μL of $Ru(bpy)_3^{2+}$ (40 mM) were mixed with constant magnetic stirring to form the water-in-oil microemulsion. After addition of 100 μL of tetraethyl orthosilicate (TEOS) and 60 μL of NH_4OH, the hydrolysis reaction was allowed to continue for 24 h. Acetone was then added to destroy the emulsion, followed by centrifuging and washing with ethanol and water. The obtained orange-colored RuSi NPs were treated with 10% APTES alcoholic solution for 2 h to form amino group functionalized RuSi NPs. The nanoparticles were then rinsed with ethanol to remove loosely bound APTES and resuspended in PBS. A 500 μL sample of $Ru(bpy)_3^{2+}$−NHS was added into the above RuSi NP solution with the same volume under stirring at room temperature, and the surface modification was allowed to proceed for 24 h. RuSi@$Ru(bpy)_3^{2+}$ NPs were obtained after being collected by centrifugation and washed several times with PBS to remove excess $Ru(bpy)_3^{2+}$. Then 2.5% (v/v) glutaraldehyde (GA) in PBS was added into the RuSi@ $Ru(bpy)_3^{2+}$ solution for 2 h of incubation at room temperature. After careful washing with PBS, the GA modified RuSi@ $Ru(bpy)_3^{2+}$ was employed for antisense DNA labeling.

Fabrication of the Microfluidic Channel and ITO Microelectrode. Glass molds with positive surface reliefs were prepared according to a previous report and used as molds for the preparation of the PDMS microfluidic channel and U-shaped ITO microelectrode.[12] Briefly, a mask with a predesigned micropattern (straight line or U-shaped curve) was placed on an SG-2506 borosilicate glass and exposed to UV radiation, followed by developing with a 0.5% NaOH solution. The Cr layer was then removed by a 0.2 M ammonium cerium(IV) nitrate solution. Etching of these glass plates was carried out in a water bath with a 1 M HF−NH_4F solution (40 °C) for 45 min. After that, positive relief channel structures were obtained. Then degassing PDMS was cast on the glass molds for 30 min at 80 °C. After cooling, the PDMS was peeled from the mold.

The as-prepared U-shaped PDMS microchannel (arms 500 μm width, spacing 1.5 cm) was attached to the ITO substrate (4 cm × 4 cm) to fabricate the ITO microelectrode. NaOH (1 M) was introduced into the microchannel for 1 h to ensure the presence of hydroxyl groups on the ITO glass surface. The microchannel was then rinsed with water and dried at 80 °C for 30 min. Thereafter, the microchannel was filled with carbon ink and allowed to dry in a thermostat at 30 °C for 30 min. The PDMS mold was peeled off, leaving corresponding patterns on the ITO substrate. Finally, the exposed ITO surface was etched with an aqueous acid solution ($FeCl_3$:HNO_3:HCl = 0.5 M:1 M:1 M), and the remaining ink was removed with ethanol. The prepared ITO microelectrode is shown in Scheme 1.

The as-prepared PDMS slice with a straight microchannel (3.5 cm long, 500 μm wide, and 45 μm high) was reversibly aligned with a glass substrate onto which the U-shaped ITO microelectrode has been microfabricated. The direction of the microchannel was perpendicular to that of the U-shaped ITO microelectrode.

Fabrication of the ECL DNA Sensor. The antisense DNA modified ITO microelectrode was prepared according to previously reported literature with minor modifications.[18] The as-prepared U-shaped ITO microelectrode was immersed in an ethanol solution of APTES (5%, v/v) overnight to form a reactive amine on the surface of the ITO microelectrode. Then it was thoroughly rinsed with ethanol to remove loosely bound molecules and heated at 80 °C for 10 min. This amine group modified ITO microelectrode was irreversibly embedded into the as-prepared straight PDMS microchannel (3.5 cm long, 500 μm wide, and 45 μm high) for the following fabrication of the ECL biosensor. Two holes (~1.5 mm) were punched at both ends of the PDMS microchannel as reservoirs. GA, as a cross-linker between the ITO electrode and DNA, was pipetted into the left reservoir. GA solution flowed through the left arm of the U-shaped microelectrode, and then ultrapure water was injected into the right reservoir to form an air chamber in the microchannel which prevented the GA solution from going into the right arm of the U-shaped microelectrode. After incubation with GA for 2 h at 37 °C, the microchannel was carefully rinsed with PBS. Antisense DNA (1×10^{-7} M) in PBS (0.1 M, pH 7.4, 0.1 M NaCl) was introduced into the microchannel and incubated for 3 h at 37 °C. After rinsing with ultrapure water for 30 s to get rid of salts, the stem−loop structure of antisense DNA was converted into linear ssDNA,[19] allowing the modification of RuSi@$Ru(bpy)_3^{2+}$ probes on antisense DNA. The antisense DNA modified electrode was conjugated with the GA modified RuSi@$Ru(bpy)_3^{2+}$ probe and incubated for 2 h at 37 °C, and then the unoccupied sites of GA were blocked with 2% BSA for 30 min. The microchannel was rinsed with PBS and incubated with the high-salt PBS solution for 1 h to remove the nonspecifically binding RuSi@$Ru(bpy)_3^{2+}$ and reduce the electrostatic repulsion between the negative charges on the DNA backbone which brought RuSi@$Ru(bpy)_3^{2+}$ close to the electrode surface.[20,21]

ECL Measurement. The ECL measurement was performed on an MPI-E multifunctional electrochemical and chemilumi-

dx.doi.org/10.1021/ac3009912 | Anal. Chem. 2012, 84, 5407−5414

Scheme 1. Schematic Representation of Intracellular c-Myc mRNA Detection Based on the Wireless ECL Biosensor

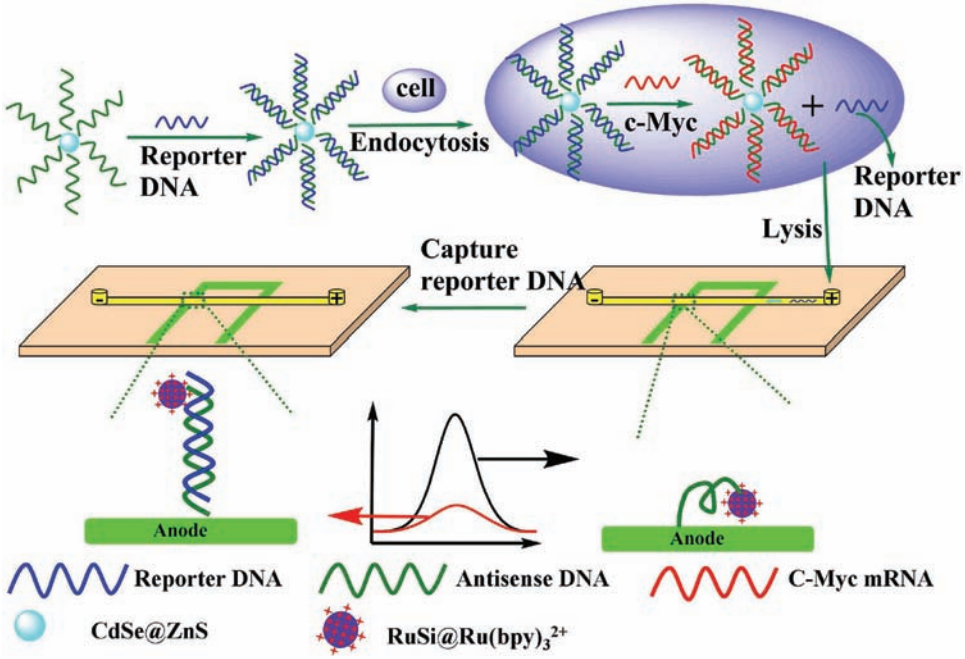

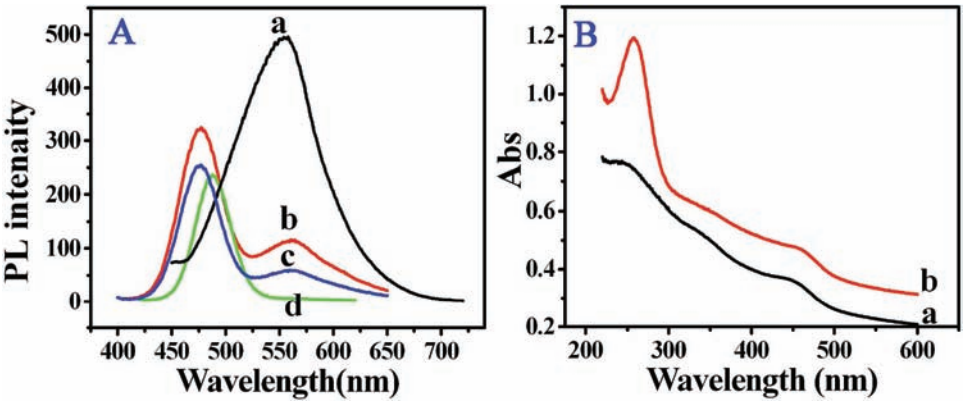

Figure 1. (A) PL spectra of CdSe@ZnS core/shell QDs with tuned ZnS layer thickness. The reaction time was 0 h (a), 0.5 h (b), 2 h (c), and 5 h (d). (B) Absorption spectra of CdSe@ZnS core/shell QDs (a) and CdSe@ZnS−dsDNA conjugates (b).

nescent analytical system. The potential bias applied between the two reservoirs (platinum wire electrodes) was generated by a 660A electrochemical workstation (CH Instruments, China). The sensors were incubated with different concentrations of reporter DNA at 37 °C for 40 min before being monitored using ECL measurements with a linear potential from 1 to 3.5 V. Regenerations of the DNA biosensor were obtained via rinsing with ultrapure water for 30 s at room temperature.

RESULTS AND DISCUSSION

Detection Principle. Here, we report a new ECL biosensor for sensitive detection of intracellular mRNA without the calibration with pure mRNA. The procedures are schematically depicted in Scheme 1. Approaches for delivery of oligonucleotides into cells have been proven to be a major challenge for intracellular detection. The cellular internalization of oligonucleotide-based probes typically requires transfection carriers that are nontoxic and cannot alter cellular processes. Here, CdSe@ZnS QD−dsNDA conjugates provided an intracellular hybridization process that correlated with the relative levels of intracellular c-Myc mRNA. The biorecognition element of c-Myc mRNA consisted of antisense DNA probe modified CdSe@ZnS QDs that were complementary to the c-Myc mRNA transcript covering the region from 947 to 966 bp. CdSe@ZnS−antisense DNA was then allowed to hybridize with reporter DNA which could be displaced by the c-Myc mRNA target (Scheme 1). In this design, c-Myc mRNA was captured on the CdSe@ZnS QD surface through the hybridization of antisense DNA, which caused blocking of protein translation and apoptosis of tumor cells. Consequently, reporter DNA was liberated from cell lysates and detected by the ECL biosensor. In this study, we employed BPE to capture and detect the released reporter DNA from CdSe@ZnS−dsDNA transfected cells and then evaluate the expression level of intracellular c-Myc mRNA. The designed on-chip wireless ECL biosensor is shown in Scheme 1. Antisense DNA was attached to the left pole of the U-shaped BPE and covalently linked to RuSi@Ru(bpy)$_3^{2+}$ probes. When the external voltage (E_{tot}) applied on the two ends of the microchannels reached a critical value, the redox reaction took place at both arms of the

dx.doi.org/10.1021/ac3009912 | Anal. Chem. 2012, 84, 5407−5414

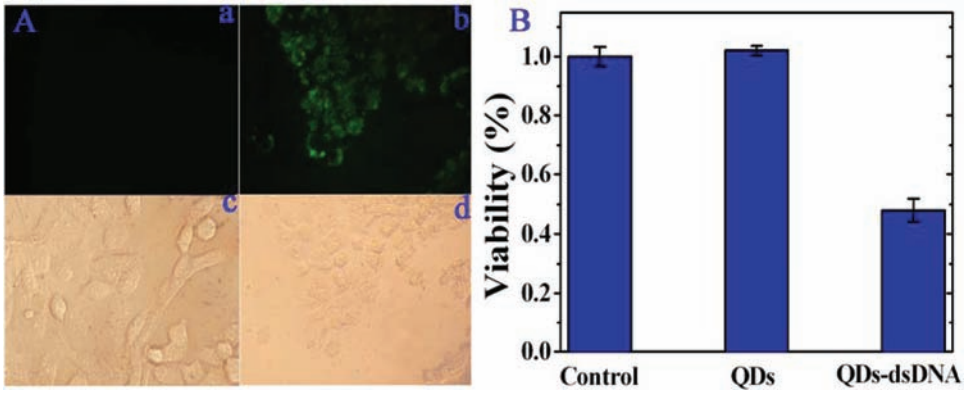

Figure 2. (A) Fluorescence images (a, b) and bright field images (c, d) of MCF-7 cells after treatment without (a, c) and with (b, d) CdSe@ZnS–dsDNA for 2 h. (B) Viability of MCF-7 cell lines treated without (control) and with CdSe@ZnS QDs and CdSe@ZnS–dsDNA conjugates.

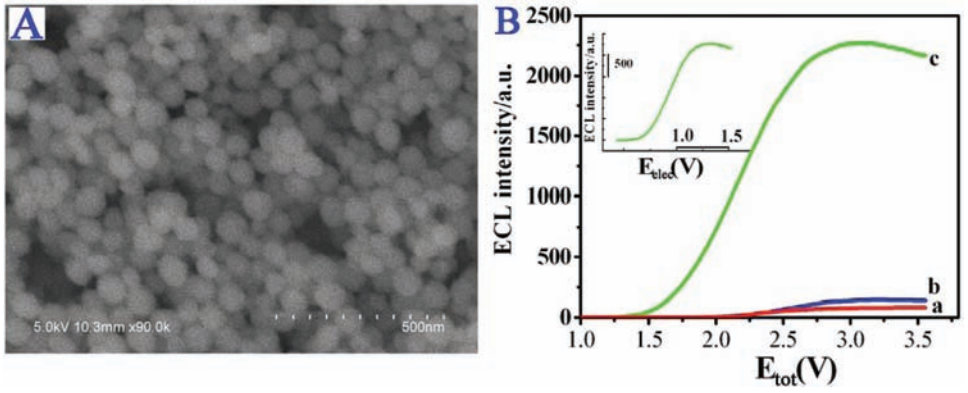

Figure 3. (A) SEM image of RuSi@Ru(bpy)$_3^{2+}$ nanoparticles. (B) ECL profiles of Ru(bpy)$_3^{2+}$–NHS (a), RuSi NP (b), and RuSi@Ru(bpy)$_3^{2+}$ NP (c) labeled antisense DNA. The inset shows the relationship between E_{elec} and the ECL intensity of RuSi@Ru(bpy)$_3^{2+}$ NP labeled antisense DNA.

U-shaped BPE simultaneously. The potential difference (ΔE_{elec}) applied on the BPE was calculated by the following equation:

$$\Delta E_{elec} = \frac{E_{tot}}{l_{channel}} l_{elec} \quad (1)$$

Here, $l_{channel}$ is the length of the microchannel and l_{elec} is the distance between the two arms of the U-shaped BPE. In the absence of reporter DNA, RuSi@Ru(bpy)$_3^{2+}$ was brought into close proximity of the electrode surface because of the flexibility of the ssDNA molecule;[22] then a strong ECL emission could be observed when the microchannel was filled with the coreactant TPA. Upon hybridization to the reporter DNA target, the formation of a rigid rodlike structure of dsDNA caused RuSi@Ru(bpy)$_3^{2+}$ to be located away from the electrode, leading to a decrease of the ECL signal.

Characterization of CdSe@ZnS QDs and Their Cytotoxicity Test. c-Myc mRNA in MCF-7 cells was used as a model target for the demonstration of the proof of concept. By utilizing CdSe@ZnS QDs, dsDNA did not require the microinjection technique to enter cells and the cytotoxic effects of QD carriers could be decreased by a ZnS shell on the CdSe core to form a core/shell structure. Figure 1A shows the photoluminescence (PL) spectra of the CdSe@ZnS core/shell system with different synthesis times. The PL peak of CdSe appeared at 550 nm (curve a), whereas a new PL peak around 470 nm was observed during the formation of the CdSe@ZnS core/shell at different reaction times (curves b–d). The decreasing PL value around 550 nm was attributed to the surface deep trap of CdSe and disappeared after the ZnS outer coating for a reaction time of 5 h, which was consistent with the core/shell formation. This CdSe@ZnS QD was then conjugated with dsDNA for delivery of oligonucleotides into cells. Figure 1B demonstrated the absorption spectra of bare CdSe@ZnS QDs (curve a) and CdSe@ZnS–dsDNA conjugates (curve b). It can be seen that CdSe@ZnS QDs showed a shoulder absorption around 450 nm, while CdSe@ZnS–dsDNA conjugates exhibited a new band at 260 nm which showed that dsDNA was successfully conjugated onto the surface of CdSe@ZnS QDs.

To validate the CdSe@ZnS–dsDNA conjugate internalization into cells, a DMIRE2 inverted fluorescence microscope was utilized to capture the fluorescence images of cells using MCF-7 cells as a model. Figure 2A showed fluorescence images for cells treated without (a) and with (b) CdSe@ZnS–dsDNA for 2 h. It can be seen that CdSe@ZnS–dsDNA conjugate transfected cells exhibited high fluorescence signals as compared to the controls (a), clearly suggesting the endocytosis of CdSe@ZnS–dsDNA conjugates into MCF-7 cells. Next, we evaluated the cytotoxicity of these CdSe@ZnS–dsDNA conjugates with bright field microscopy based on the changes in cell morphology after treatment without (c) and with (d) CdSe@ZnS–dsDNA conjugates. As shown in Figure 2A (curves c and d), we observed the shrinkage of MCF-7 cells and the formation of an apoptotic body after treatment with CdSe@ZnS–dsDNA conjugates. These results indicated that CdSe@ZnS–dsDNA conjugates could effectively induce cell death. To demonstrate the apoptosis of MCF-7 cells is induced

dx.doi.org/10.1021/ac3009912 | Anal. Chem. 2012, 84, 5407–5414

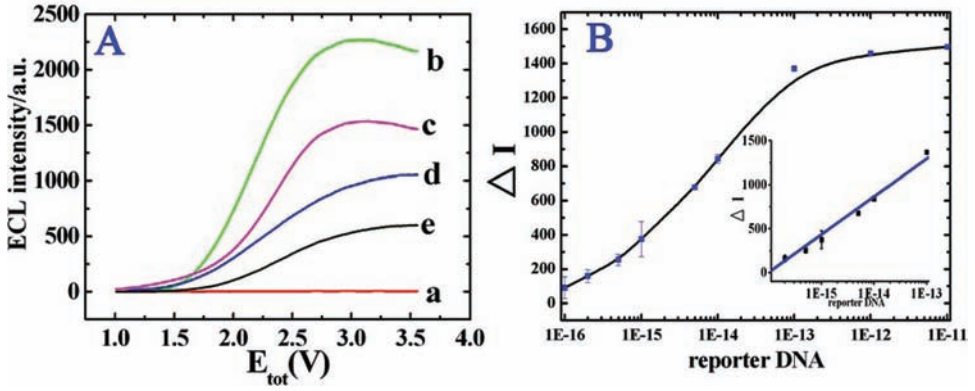

Figure 4. (A) ECL−E_{tot} curves for the antisense DNA modified ITO electrode (a) and RuSi@Ru(bpy)$_3^{2+}$−antisense DNA modified ITO electrode in the presence of reporter DNA with different contentrations (from b to e): 0, 6×10^{-15}, 6×10^{-14}, and 1×10^{-8} M reporter DNA. (B) ΔI as a function of the concentrations of reporter DNA from 1×10^{-16} to 1×10^{-11} M. The inset shows the linear fit plot of ΔI as a function of the logarithm of the reporter DNA concentration from 1×10^{-16} to 1×10^{-13} M. The error bars represent the standard deviation of three independent measurements.

by a dsDNA-induced gene-silencing effect, we conducted gene-silencing studies in MCF-7 cells after incubation without and with CdSe@ZnS QDs and CdSe@ZnS−dsDNA conjugates (Figure 2B). Cell viability was examined using an MTT assay, which is a characteristic feature of cells undergoing apoptosis, and calculated by the following equation:

$$\text{cell viability}\ (\%) = (A_{\text{test}}/A_{\text{control}}) \times 100 \qquad (2)$$

where A_{control} is obtained in the absence of QDs and A_{test} is obtained in the presence of QDs. Our results showed that CdSe@ZnS QDs were not toxic to MCF-cells. This was attributed to the protection of the ZnS shell on the CdSe QD surface, which prevented the release of toxic Cd^{2+} into MCF-7 cells. As expected, CdSe@ZnS−dsDNA conjugates were severely toxic to MCF-7 cells after 2 h due to the successful hybridization of c-Myc mRNA to CdSe@ZnS−antisense DNA, which induced the down-regulation of the c-Myc gene and steric blocking of protein translation.

Characterization of RuSi@Ru(bpy)$_3^{2+}$ NPs and Their Signal Amplification Effect. Figure 3A shows the morphologies of RuSi@Ru(bpy)$_3^{2+}$ NPs by using scanning electron microscopy (SEM). According to the SEM observation, the as-prepared RuSi@Ru(bpy)$_3^{2+}$ NPs were highly monodisperse and had an average diameter of about 50 nm. ECL performance of RuSi@Ru(bpy)$_3^{2+}$−antisense DNA on BPE was also investigated, and the results are shown in Figure 3B (curve c). It can be seen that the RuSi@Ru(bpy)$_3^{2+}$−antisense DNA modified electrode displayed a relatively strong ECL signal, suggesting the successful labeling of ECL tags on antisense DNA. It exhibited a clear ECL peak at 2.8 V (ΔE_{tot}) on the ITO BPE which corresponded to the ECL reaction resulting from the oxidation of Ru(bpy)$_3^{2+}$ and TPA at the anodic pole of BPE. At the same time, the electrocatalytic reduction of O_2 took place at the cathodic pole of the BPE. The potential difference (ΔE_{elec}) was calculated to be ca. 1.2 V (inset in Figure 3B) by the above-mentioned equation.

To gain a better understanding of signal amplification of RuSi@Ru(bpy)$_3^{2+}$ probes, comparison experiments were carried out in which antisense DNA was labeled with RuSi NPs (curve b) and Ru(bpy)$_3^{2+}$−NHS (curve a), respectively, shown in Figure 3B. Both of them exhibited an ECL peak at ca. 2.8 V. In comparison with RuSi and Ru(bpy)$_3^{2+}$−NHS, RuSi@Ru(bpy)$_3^{2+}$ provided an approximately 12-fold and 24-fold ECL enhancement, respectively. The large increase of ECL emission intensity was attributed to the large loading of Ru(bpy)$_3^{2+}$ onto silica carriers, which could react with TPA and greatly enhance the ECL signal. Thus, RuSi@Ru(bpy)$_3^{2+}$ was a more efficient candidate for the following ECL bioassays.

ECL Response of Reporter DNA. Important experimental parameters, including the hybridization time and assembly time of antisense DNA, were investigated before the detection of reporter DNA, and the results are shown in Figures S1 and S2 in the Supporting Information, respectively. It can be seen from Figure S1 that the decrement of ECL intensity ($\Delta I = I_0 - I$, where I_0 and I are the ECL intensities before and after hybridization, respectively) tended to increase rapidly within 20 min and then achieved equilibrium at about 30 min. Therefore, a hybridization time of 30 min was chosen in the following experiments to obtain a high sensitivity. Figure S2 shows that ΔI increased as the self-assembly time increased and reached the maximum at about 3 h. Thus, 3 h was used as the optimized self-assembly time for antisense DNA.

In the present strategy, antisense DNA was labeled with a large amount of Ru(bpy)$_3^{2+}$ corresponding to one reporter DNA. Therefore, a high amplification factor of Ru(bpy)$_3^{2+}$ for each reporter DNA molecule can be achieved. As shown in Figure 4A, no ECL signals could be observed on the antisense DNA modified ITO electrode (curve a), while the RuSi@Ru(bpy)$_3^{2+}$−antisense DNA modified electrode surface displayed a relatively strong ECL signal (curve b). After addition of reporter DNA into this system, the ECL intensity obviously decreased with an increase of the reporter DNA concentration (curves c−e), confirming the separation of RuSi@Ru(bpy)$_3^{2+}$ tags from the ITO electrode through the hybridization of reporter DNA and antisense DNA. Thus, quantifying the reporter DNA concentration can be carried out by monitoring the changes in the ECL signal. The sensitivity and the quantitative behavior of the ECL biosensors were assessed by measuring the dependence of ΔI upon reporter DNA at different concentrations (Figure 4B). This clearly demonstrated that the addition of reporter DNA at different concentrations to the sensing system induced different increases of ΔI, associated with the decreasing amount of RuSi@Ru(bpy)$_3^{2+}$ in close proximity to the ITO BPE. As expected, ΔI increased along with the increasing reporter DNA concentration ranging from 2×10^{-16} to 1×10^{-11} M. The inset in Figure 4B shows that the

dx.doi.org/10.1021/ac3009912 | Anal. Chem. 2012, 84, 5407−5414

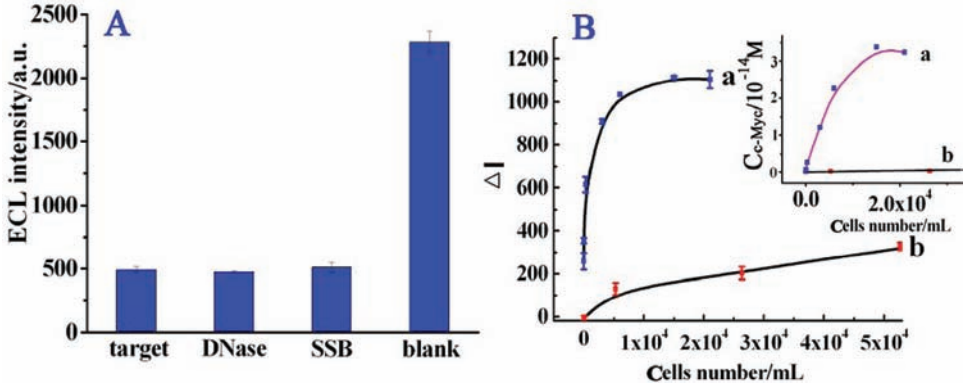

Figure 5. (A) ECL signals of RuSi@Ru(bpy)$_3^{2+}$−antisense DNA in response to reporter DNA (1×10^{-7} M) without and with SSB (1 nM) or DNase I (1 nM). (B). Cell-associated ΔI of CdSe@ZnS−dsDNA transfected cells plotted as a function of the c-Myc concentration in MCF-7 cells (a) and LO2 cells (b). The inset shows the relationship between the cell number and cellular c-Myc concentration in MCF-7 cells (a) and LO2 cells (b).

response signal was logarithmically proportional to the reporter DNA concentration ranging from 1×10^{-16} to 1×10^{-13} M with a linear correlation ($R^2 = 0.9906$). The experimental data demonstrated the ultrahigh sensitivity of this strategy and reflected the high signal amplification of RuSi@Ru(bpy)$_3^{2+}$ NPs.

Measurement of the c-Myc mRNA Expression Level in Cells. DNA is known to bind single-stranded DNA binding protein (SSB) sequence-nonspecifically[23] and be degraded by enzymes such as DNase I,[24] both of which would give false-positive signals for quantitative detection. To demonstrate that the proposed ECL biosensor can be used to quantify intracellular c-Myc mRNA, we first examined whether nonspecific protein interactions and enzymatic degradation could be responsible for generating false-positive signals. We incubated RuSi@Ru(bpy)$_3^{2+}$−antisense DNA without and with SSB (1 nM) and DNase I (1 nM) in the presence of reporter DNA and then observed the ECL signal changes. As can be seen in Figure 5A, the ECL intensity presented a significant decrease in the presence of the target (reporter DNA). When SSB/reporter DNA and DNase I/reporter DNA were introduced into the microchannel, no significant ECL changes were observed on the antisense DNA modified electrode when compared with the ECL signal obtained without SSB and DNase I. The stability may be due to steric hindrance of nanoparticles and high salt concentration, which can provide good protection of DNA from nuclease digestion or SSB interaction.[24]

Then we conducted intracellular hybridization experiments to quantitatively assay the expression level of c-Myc mRNA by transfection of CdSe@ZnS−dsDNA into MCF-7 cells. The c-Myc mRNA expression level in cells could be measured through quantification of reporter DNA. To quantify cellular c-Myc mRNA levels, reporter DNA in lysed solution was measured by the prepared ECL biosensor. The c-Myc mRNA in LO2 cell lines was used as a control. Levels of c-Myc gene were determined relative to the released reporter DNA from CdSe@ZnS QDs. [c-Myc$_{cellular}$] = [DNA$_{reporter}$]/total cell population, and the results are shown in Figure 5B. Curve a shows that cell-associated ΔI corresponds to cellular c-Myc mRNA levels ranging from 3.0 to 2.1×10^4 cells/mL. When the cell number increases to 1.5×10^4 /mL, the curve begins to level off due to the saturation of reporter DNA at the highest intracellular c-Myc mRNA concentrations. Quantitative detection revealed that the average copy number of c-Myc mRNA per MCF-7 cell was 2203 ± 256 (inset in Figure 5B, curve a), which is at the same level as that in a previous report (2907 ± 289 c-Myc transcripts in each MCF-7 cell).[25] As a control, LO2 cells displayed a very slow increment of ΔI ranging from 52 to 5.2×10^4 cells/mL (curve b), and the relationship between LO2 cell number and c-Myc concentration is shown in the inset of Figure 5B. c-Myc mRNA in the LO2 cell was calculated to be 13 ± 2 copies. The overall set of observations demonstrated that the antisense DNA based ECL sensor can be used to sensitively quantify the intracellular c-Myc gene without further amplification of the c-Myc gene.

Besides selectivity and sensitivity, reusability is also an important feature for biosensors. Regeneration of the ECL biosensor was achieved by introducing ultrapure water into the microchannel for 30 s, which disrupts the hybridization.[19] We found that the prepared ECL biosensor could be conveniently regenerated over 15 cycles with a recovery of >95% of the original signal.

CONCLUSIONS

We presented an accurate and sensitive method for quantitatively monitoring a genetic marker in the mRNA population in tumor cells and simultaneously investigating the apoptosis of tumor cells on the basis of a wireless on-chip ECL system. The use of RuSi@Ru(bpy)$_3^{2+}$ for signal amplification showed a 24-fold improvement in assay sensitivity with respect to single-molecule labels (Ru(bpy)$_3^{2+}$−NHS), which enabled the detection of reporter DNA at 10^{-16} M levels. Furthermore, CdSe@ZnS−dsDNA readily entered into cells where it can be used to detect cellular c-Myc RNA levels and investigate the apoptosis mechanism of tumor cells, which makes it an excellent candidate for cellular gene detection and diagnosis. Our results demonstrated that decreases in c-Myc levels can inhibit tumor cell growth. The sensitivity and time-saving features make this an attractive approach for molecular detection of other cancer cells that may play a role in disease diagnosis.

ASSOCIATED CONTENT

Supporting Information

Additional information as noted in text. This material is available free of charge via the Internet at http://pubs.acs.org.

dx.doi.org/10.1021/ac3009912 | Anal. Chem. 2012, 84, 5407−5414

AUTHOR INFORMATION

Corresponding Author

*Phone/fax: +86-25-83597294. E-mail: xujj@nju.edu.cn.

Notes

The authors declare no competing financial interest.

ACKNOWLEDGMENTS

This work was supported by the 973 Program (Grant 2012CB932600), the National Natural Science Foundation (Grants 21025522, 20890020, and 21135003), and the National Natural Science Funds for Creative Research Groups (Grant 21121091).

REFERENCES

(1) Kauraniemi, P.; Bärlund, M.; Monni, O.; Kallioniemi, A. *Cancer Res.* **2001**, *61*, 8235−8240.
(2) Stephen, S. W.; Yeung, T. M. H. L.; I-Ming, Hsing. *Anal. Chem.* **2008**, *80*, 363−368.
(3) Vandevyver, C.; Motmans, K.; Raus, J. *Genome Res.* **1995**, *5*, 195−201.
(4) Baeumner, A. J.; Humiston, M. C.; Montagna, R. A.; Durst, R. A. *Anal. Chem.* **2001**, *73*, 1176−1180.
(5) Lo, W.-Y.; Baeumner, A. J. *Anal. Chem.* **2007**, *79*, 1548−1554.
(6) Perlette, J.; Tan, W. *Anal. Chem.* **2001**, *73*, 5544−5550.
(7) Santangelo, P.; Nitin, N.; Bao, G. *Ann. Biomed. Eng.* **2006**, *34*, 39−50.
(8) Medley, C. D.; Drake, T. J.; Tomasini, J. M.; Rogers, R. J.; Tan, W. *Anal. Chem.* **2005**, *77*, 4713−4718.
(9) Li, J.; Yang, L.; Luo, S.; Chen, B.; Li, J.; Lin, H.; Cai, Q.; Yao, S. *Anal. Chem.* **2010**, *82*, 7357−7361.
(10) Chow, K.-F.; Chang, B.-Y.; Zaccheo, B. A.; Mavré, F. o.; Crooks, R. M. *J. Am. Chem. Soc.* **2010**, *132*, 9228−9229.
(11) Zhan, W.; Alvarez, J.; Crooks, R. M. *J. Am. Chem. Soc.* **2002**, *124*, 13265−13270.
(12) Wu, M.-S.; Xu, B.-Y.; Shi, H.-W.; Xu, J.-J.; Chen, H.-Y. *Lab Chip* **2011**, *11*, 2720−2724.
(13) Wang, Y.-h.; Liu, S.; Zhang, G.; Zhou, C.-Q.; Zhu, H.-X.; Zhou, X.-B.; Quan, L.-P.; Bai, J.-F.; Xu, N.-Z. *Breast Cancer Res.* **2005**, *7*, R220.
(14) Wang, X. Y.; Zhou, J. M.; Yun, W.; Xiao, S. S.; Chang, Z.; He, P. G.; Fang, Y. Z. *Anal. Chim. Acta* **2007**, *598*, 242−248.
(15) Yang, F. F.; Yu, J. S.; Xie, Y. *Chin. J. Inorg. Chem.* **2008**, *24*, 1142−1147.
(16) Shi, Z. X.; Wang, Y. F.; Liu, J. J; Yang, R. Q.; Zuo, S. L.; Yu, Y. C. *Chin. J. Inorg. Chem.* **2008**, *24*, 1186−1190.
(17) Zabzdyr, J. L.; Lillard, S. J. *Anal. Chem.* **2002**, *74*, 1857−1862.
(18) Lei, K. F. *Meas. Sci. Technol.* **2011**, *22*, 105802.
(19) Lubin, A. A.; Lai, R. Y.; Baker, B. R.; Heeger, A. J.; Plaxco, K. W. *Anal. Chem.* **2006**, *78*, 5671−5677.
(20) Steel, A. B.; Herne, T. M.; Tarlov, M. J. *Anal. Chem.* **1998**, *70*, 4670−4677.
(21) Murphy, M. C.; Rasnikl, I.; Cheng, W.; Lohman, T. M.; Ha, T. *Biophys. J.* **2004**, *86*, 2530−2537.
(22) Anne, A.; Bouchardon, A.; Moiroux, J. *J. Am. Chem. Soc.* **2003**, *125*, 1112−1113.
(23) Al-Mahrouki, A. A.; Krylov, S. N. *Anal. Chem.* **2005**, *77*, 8027−8030.
(24) Lohman, T. M.; Overman, L. B.; Datta, S. *J. Mol. Biol.* **1986**, *187*, 603−615.
(25) Chen, A. K.; Behlke, M. A.; Tsourkas, A. *Nucleic Acids Res.* **2007**, *35*, e105.